Figure S1

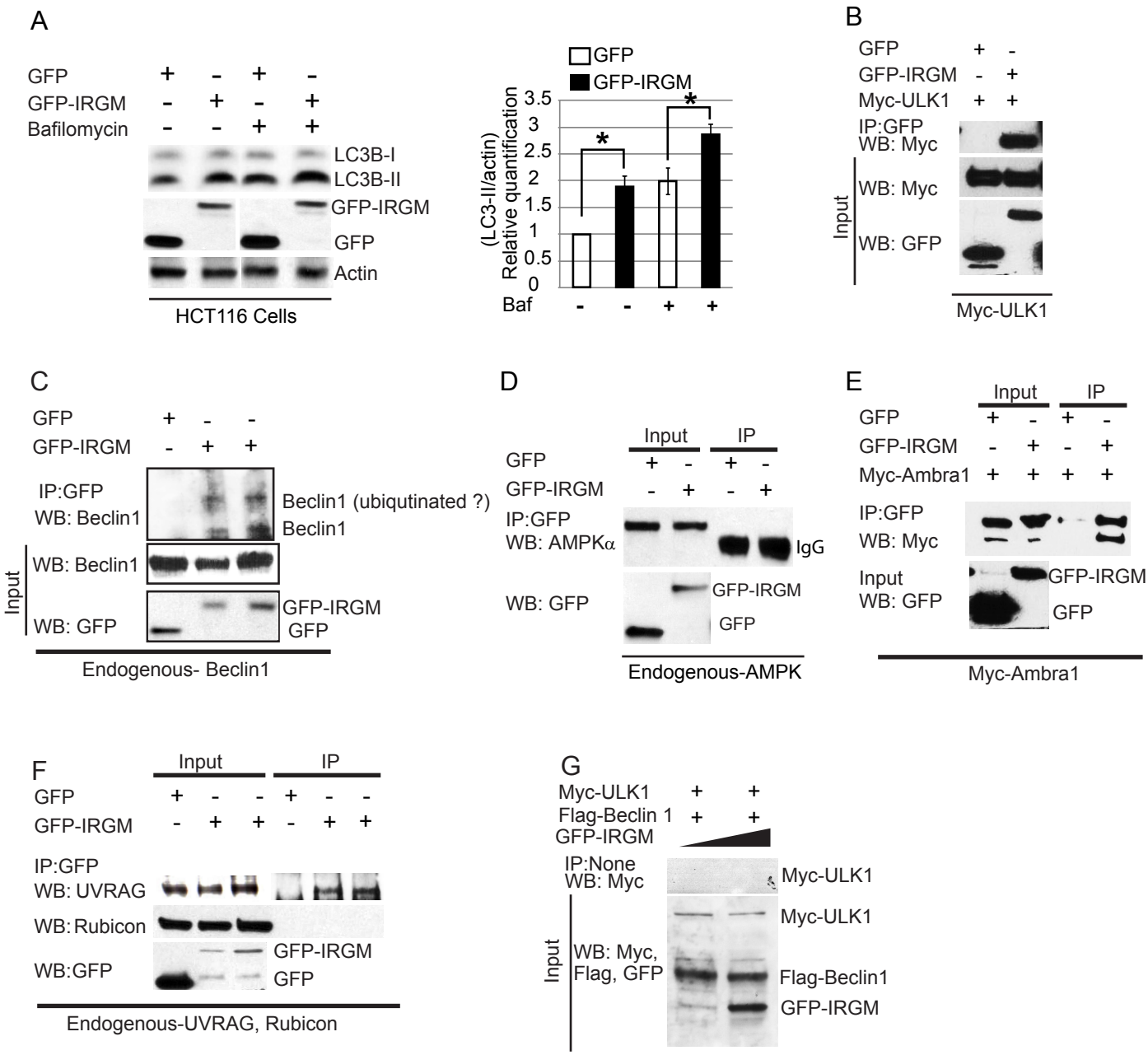

Figure S1, related to Fig. 1. IRGM interacts with core autophagy machinery. (**A**) Left panel, Western blotting with lysates of bafilomycin (100 nM, 2 h) treated or untreated HCT116 cells expressing GFP or GFP-IRGM. Right panel, densitometric analysis of Western blots. Data, means ±SD (n=3); *, p>0.05 (t test). (**B**) Co-IP analysis with HEK293T cell co-expressing either GFP or GFP-IRGM and Myc-ULK1. (C-F) Co-IP experiments with HEK293T cell expressing GFP or GFP-IRGM (**C, D, F**) and Myc-AMBRA1 (**E**); Western blotting was done with indicated antibodies. (**G**) Co-IP analysis of beads alone as a control for interaction of ULK1-Beclin1 at lowest and highest IRGM protein concentrations shown in Figure 1I.

Figure S2

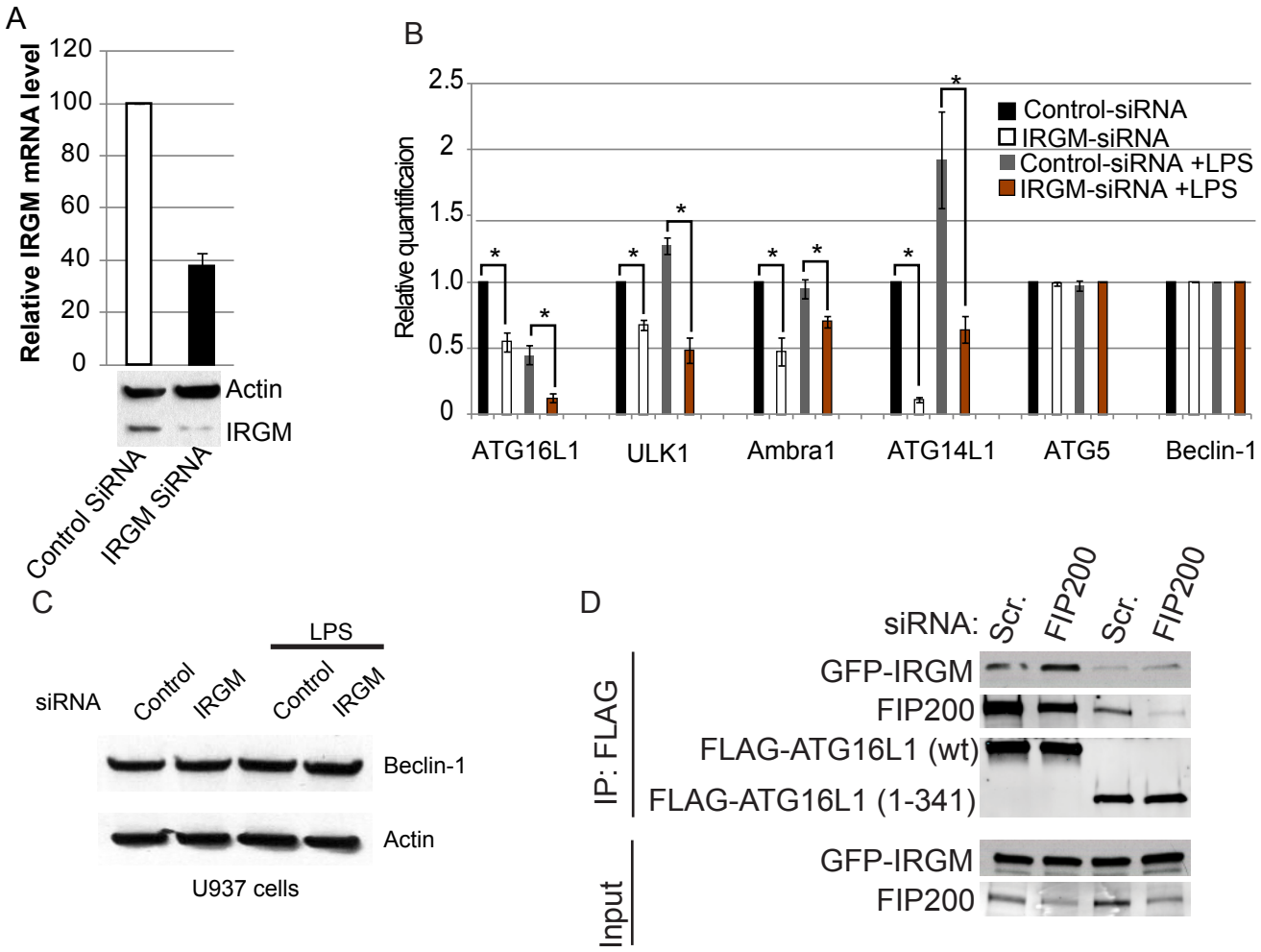

F**igure S2, related to Fig. 2. IRGM stabilizes core autophagy machinery.** (**A)** Graph and Western blot showing the knockdown efficiency of *IRGM* in U937 monocytic cells. In qRT-PCR gene expression is normalized by GAPDH. (**B**) Graph showing the densitometric analysis of Western blots in Figure 2 A, C, E. Data, means ±SD (n=3); *, p>0.05 (t test). (**C**) U937 monocyte cells transfected with control or *IRGM* siRNA, untreated or treated with LPS (500 ng/ml for 4 h) were lysed and subjected to Western blotting with indicated antibodies. (**D**) Coimmunoprecipitation analysis of the effect of FIP200 knockdown on interactions between GFP-IRGM and FLAG-ATG16L1 (wt or residues 1-341) in HEK293T cells.

Figure S3

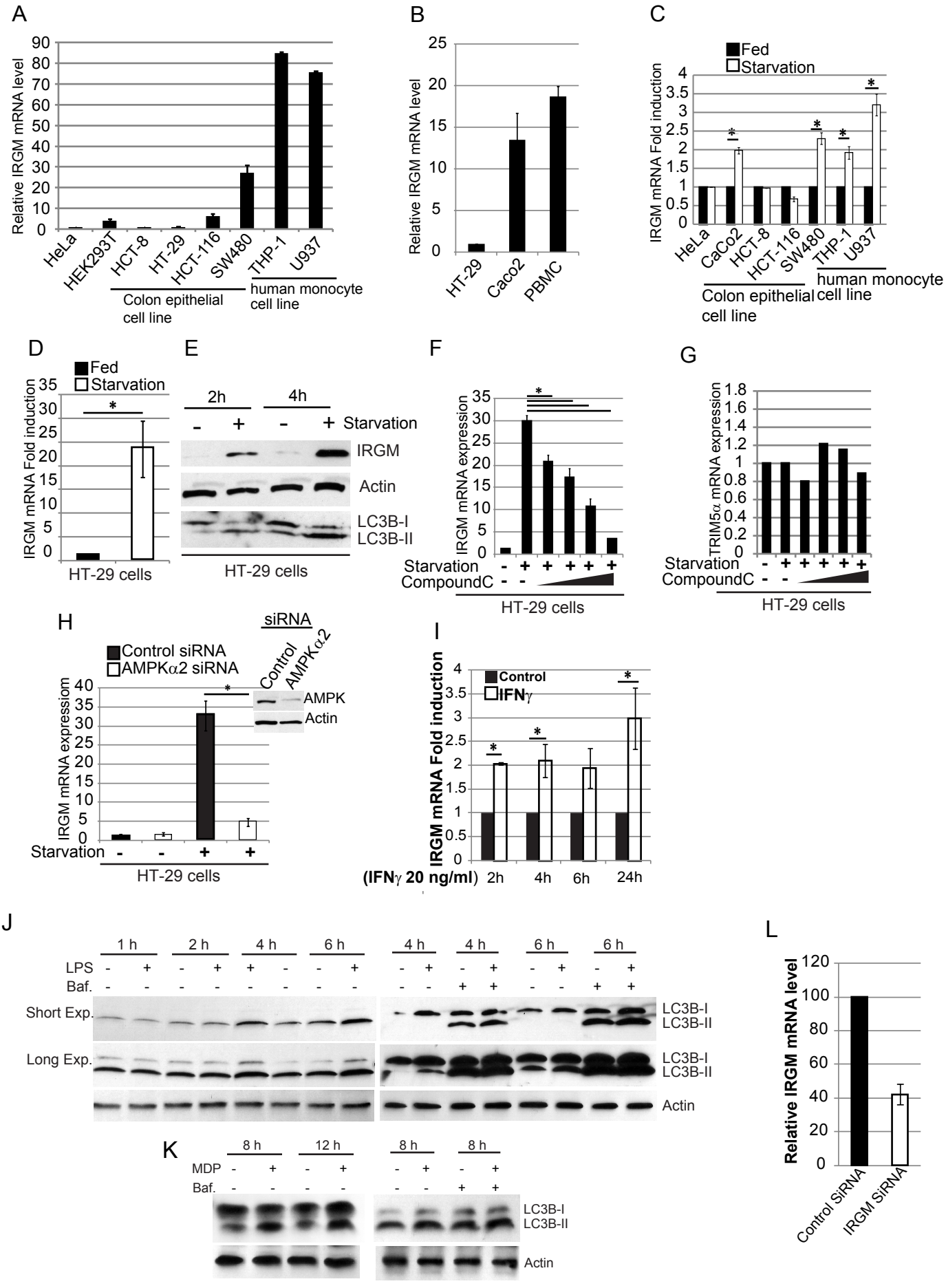
A
Relative IRGM mRNA level
HeLa
HEK293T
HCT-8
HT-29
HCT-116
SW480
THP-1
U937
Colon epithelial cell line
human monocyte cell line
B
Relative IRGM mRNA level
HT-29
Caco2
PBMC
C
Fed
Starvation
IRGM mRNA Fold induction
HeLa
CaCo2
HCT-8
HCT-116
SW480
THP-1
U937
Colon epithelial cell line
human monocyte cell line
D
Fed
Starvation
IRGM mRNA Fold induction
HT-29 cells
E
2h
4h
Starvation
IRGM
Actin
LC3B-I
LC3B-II
HT-29 cells
F
IRGM mRNA expression
Starvation
CompoundC
HT-29 cells
G
TRIM5α mRNA expression
Starvation
CompoundC
HT-29 cells
H
siRNA
Control siRNA
AMPKα2 siRNA
Control
AMPKα2
AMPK
Actin
IRGM mRNA expression
Starvation
HT-29 cells
I
Control
IFNγ
IRGM mRNA Fold induction
(IFNγ 20 ng/ml)
2h
4h
6h
24h
J
1 h
2 h
4 h
6 h
LPS
Baf.
Short Exp.
Long Exp.
LC3B-I
LC3B-II
Actin
K
8 h
12 h
MDP
Baf.
LC3B-I
LC3B-II
Actin
L
Relative IRGM mRNA level
Control SiRNA
IRGM SiRNA

Figure S3, related to Fig. 3. Starvation induces IRGM expression through AMPK. (**A, B**) Analysis of basal IRGM expression in a panel of cell lines and primary human blood mononuclear cells (PBMC) by quantitative real-time PCR (qRT-PCR). RNA isolated from fed cells were subjected to qRT-PCR. (**C, D)** Starvation induces IRGM expression in several cell lines (C), with the highest induction (20-fold) detected in HT-29 cells (D).(**E**) Western blot from fed and starved HT-29 cells lysates showing induction of IRGM and LC3B. (**F, G**) AMPK is required for starvation induced IRGM expression in HT-29 cells. (F, G) qRT-PCR using RNA isolated from fed or starved HT-29 cells, treated with increasing concentration of compound C (20, 40, 80, 160 μM); qRT-PCR was performed with IRGM (F) or TRIM5α (G) Taqman probes. (**H**) Effects of AMPKα2 knock-down on starvation-induced IRGM expression. Inset, Western blotting showing AMPKα2 knock down efficiency. (**I**) RNA isolated from U937 cells treated with IFN-γ were subjected to qRT-PCR. (**J, K**) Western blots of LPS- and MDP-treated U937 (subjected to Bafilomycin A1 or not) cell lysates. (**L**) Graph showing knockdown efficiency of IRGM in U937 monocytic cells (related to Fig. 3E-H); qRT-PCR gene expression is normalized by GAPDH. In qRT-PCR gene expression is normalized by GAPDH. Panel C, D, H, I; Data, means +/- SE, (n=3); *$p<0.05$ (t test). Panel F ; Data, means +/- SE, (n=3); *$p<0.05$ (ANOVA) .

Figure S4

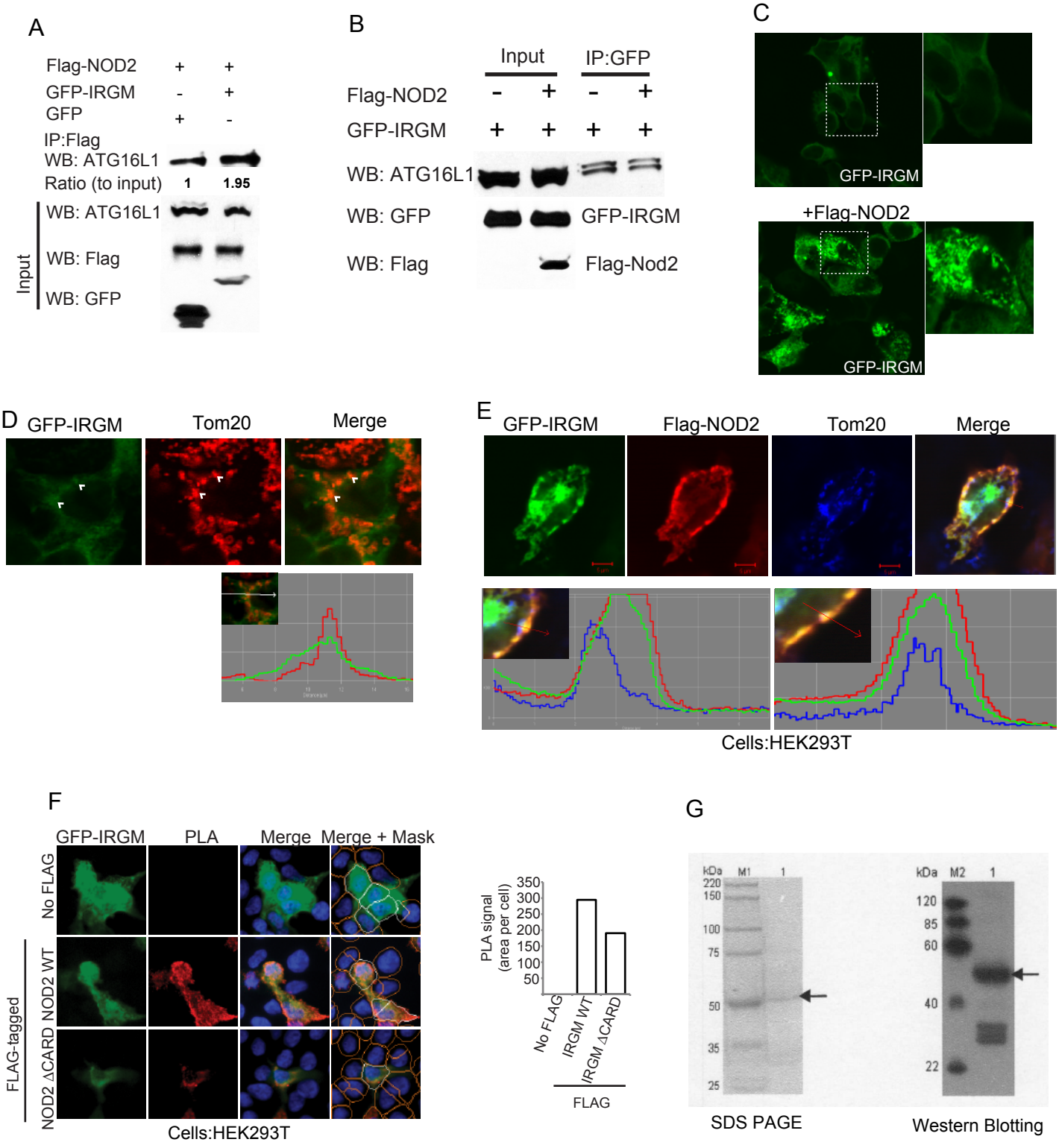
A
Flag-NOD2 + +
GFP-IRGM - +
GFP + -
IP:Flag
WB: ATG16L1
Ratio (to input) 1 1.95
Input
WB: ATG16L1
WB: Flag
WB: GFP
B
Input
IP:GFP
Flag-NOD2 - + - +
GFP-IRGM + + + +
WB: ATG16L1
WB: GFP
GFP-IRGM
WB: Flag
Flag-Nod2
C
GFP-IRGM
+Flag-NOD2
GFP-IRGM
D
GFP-IRGM
Tom20
Merge
E
GFP-IRGM
Flag-NOD2
Tom20
Merge
Cells:HEK293T
F
GFP-IRGM
PLA
Merge
Merge + Mask
No FLAG
FLAG-tagged
NOD2 WT
NOD2 ΔCARD
Cells:HEK293T
PLA signal (area per cell)
350
300
250
200
150
100
50
No FLAG
IRGM WT
IRGM ΔCARD
FLAG
G
kDa
M1
1
220
150
100
75
50
35
25
kDa
M2
1
120
85
60
40
22
SDS PAGE
Western Blotting

Figure S4, related to Fig. 4. IRGM interacts and co-localizes with ATG16L1 and NOD2. (**A**, **B**) Lysates from cells expressing GFP-IRGM and Flag-NOD2 were subjected to immunoprecipitation with anti-Flag or anti-GFP and blots were probed with antibodies as indicated. (**C**) Representative confocal images of HEK293T cells expressing GFP-IRGM alone or with NOD2. (**D, E**) HEK293T cells expressing GFP-IRGM (**D**) or GFP-IRGM and Flag-NOD2 (**E**) were subjected to immunofluorescence staining with Tom 20 (mitochondrial marker) antibody. Bottom, co-localization profile measurement along straight line using LSM 510 software. (**F**) Left panel, assessment of IRGM interactions with FLAG-NOD2 (WT and ΔCARD) by proximity ligation assay (PLA). The total area of red PLA puncta (an indication of direct protein-protein interactions) in GFP-IRGM expressing cells (white mask) was determined by high content microscopy. Nuclear labeling (blue) was used for cell identification. Orange mask, cells excluded from analysis due to GFP negativity or other pre-set criteria. Graph, average total area of PLA puncta per cell (N ≥ 500 GFP-IRGM+ cells). (**G**) SDS-PAGE and Western blot analysis of purified IRGM proteins.

Figure S5

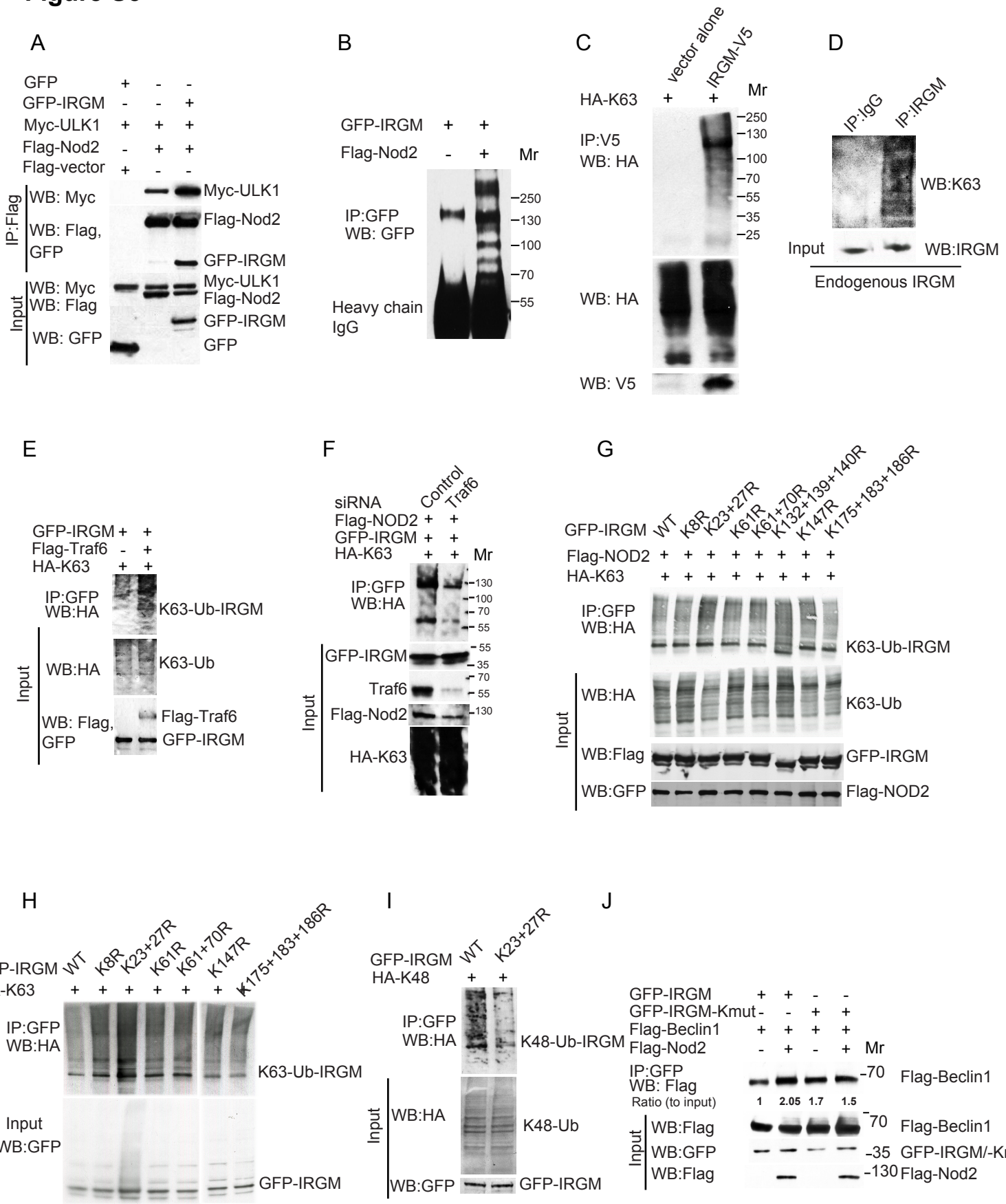
A
GFP
GFP-IRGM
Myc-ULK1
Flag-Nod2
Flag-vector
IP:Flag
WB: Myc
WB: Flag, GFP
Myc-ULK1
Flag-Nod2
GFP-IRGM
Input
WB: Myc
WB: Flag
WB: GFP
Myc-ULK1
Flag-Nod2
GFP-IRGM
GFP
B
GFP-IRGM
Flag-Nod2
Mr
IP:GFP
WB: GFP
Heavy chain
IgG
250
130
100
70
55
C
vector alone
IRGM-V5
HA-K63
Mr
IP:V5
WB: HA
WB: HA
WB: V5
250
130
100
70
55
35
25
D
IP:IgG
IP:IRGM
WB:K63
Input
WB:IRGM
Endogenous IRGM
E
GFP-IRGM
Flag-Traf6
HA-K63
IP:GFP
WB:HA
K63-Ub-IRGM
Input
WB:HA
K63-Ub
WB: Flag, GFP
Flag-Traf6
GFP-IRGM
F
siRNA
Control
Traf6
Flag-NOD2
GFP-IRGM
HA-K63
Mr
IP:GFP
WB:HA
GFP-IRGM
Traf6
Flag-Nod2
HA-K63
Input
130
100
70
55
55
35
70
55
130
G
GFP-IRGM
WT
K8R
K23+27R
K61R
K61+70R
K132+139+140R
K147R
K175+183+186R
Flag-NOD2
HA-K63
IP:GFP
WB:HA
K63-Ub-IRGM
Input
WB:HA
K63-Ub
WB:Flag
GFP-IRGM
WB:GFP
Flag-NOD2
H
GFP-IRGM
WT
K8R
K23+27R
K61R
K61+70R
K147R
K175+183+186R
HA-K63
IP:GFP
WB:HA
K63-Ub-IRGM
Input
WB:GFP
GFP-IRGM
I
GFP-IRGM
WT
K23+27R
HA-K48
IP:GFP
WB:HA
K48-Ub-IRGM
Input
WB:HA
K48-Ub
WB:GFP
GFP-IRGM
J
GFP-IRGM
GFP-IRGM-Kmut
Flag-Beclin1
Flag-Nod2
Mr
IP:GFP
WB: Flag
Ratio (to input)
1
2.05
1.7
1.5
70
Flag-Beclin1
Input
WB:Flag
70
Flag-Beclin1
WB:GFP
35
GFP-IRGM/-Kmut
WB:Flag
130
Flag-Nod2

Figure S5, related to Fig. 5. NOD2 enhances ubiquitination of IRGM. (**A**) HEK293T cell lysates expressing the indicated set of proteins were subjected to immunoprecipitation (IP) with Flag antibody and immunoblotted with antibodies as indicated (WB, Western blot). (**B**) HEK293T cell lysates co-expressing GFP-IRGM alone or with NOD2 were subjected to immunoprecipitation (IP) with GFP antibody and immunoblotted (WB) with antibody to GFP. (**C**) HEK293T cell lysates co-expressing IRGM-V5 and HA-K63 (WB) with antibody to HA. (**D**) THP-1 cell lysates were subjected to immunoprecipitation (IP) with IRGM antibody and immunoblotted (WB) with antibody to ubiquitin (K-63 specific). (**E**) HEK293T cell lysates co-expressing GFP-IRGM and HA-K63 with or without Flag-TRAF6 were subjected to immunoprecipitation with GFP antibody and subjected to Western blotting as indicated. (**F**) TRAF6 depleted HEK293T cell lysates co-expressing GFP-IRGM and HA-K63 were subjected to immunoprecipitation with GFP antibody and subjected to Western blotting as indicated. (**G**) Lysates of cells co-expressing GFP-IRGM (WT and lysine mutants), HA-K63 and Flag-NOD2 were subjected to immunoprecipitation with anti-GFP and blot was probed with antibodies as indicated. (**H**) Lysates of cells co-expressing GFP-IRGM (WT and lysine mutants) and HA-K63 were subjected to immunoprecipitation with anti-GFP and blot was probed with antibodies as indicated. (**I**) Lysates of cells co-expressing GFP-IRGM (WT and K23/27 lysine mutants) and HA-K48 were subjected to immunoprecipitation with anti-GFP and blot was probed with antibodies as indicated. (**J**) Effect of NOD2 on IRGM/IRGM^{kmut}- Beclin 1 interactions assessed by Co-IP analyses.

Figure S6

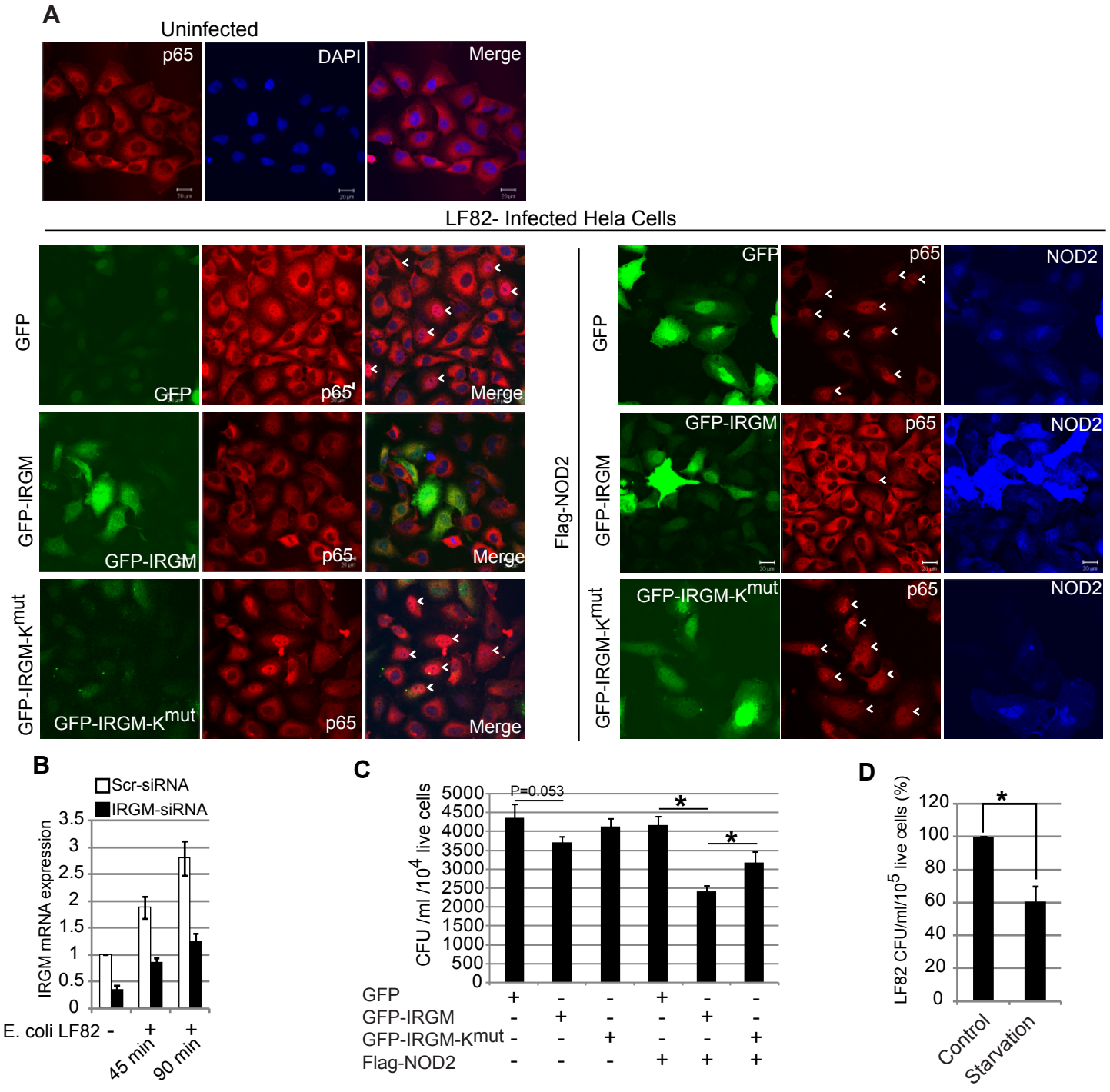

Figure S6, related to Fig. 7. Ubiquitination of IRGM is important for its anti-inflammatory and anti-microbial function . (A) Analysis of NFκB-p65 nuclear translocation following LF82 infection in HeLa cells expressing GFP or GFP-IRGM or GFP-IRGM-K^{mut} and/or Flag-NOD2. (B) Graph, knock down efficiency of IRGM in *E. coli* LF82 infected THP-1 cells. (C) Effects of IRGM (wild type or K^{mut}) expression with and without NOD2 on intracellular survival of *E. coli* LF82 at 5h post infection in HEK293T cells. Data, means +/- SE,(n=3); *p<0.05 (ANOVA). (D) Maximum capacity (starvation-induced) of the HEK293T cells for xenophagy-reduction of *E. coli* LF82 CFU. Data, means +/- SE, (n=3); *p<0.05 (t test).

Figure S7

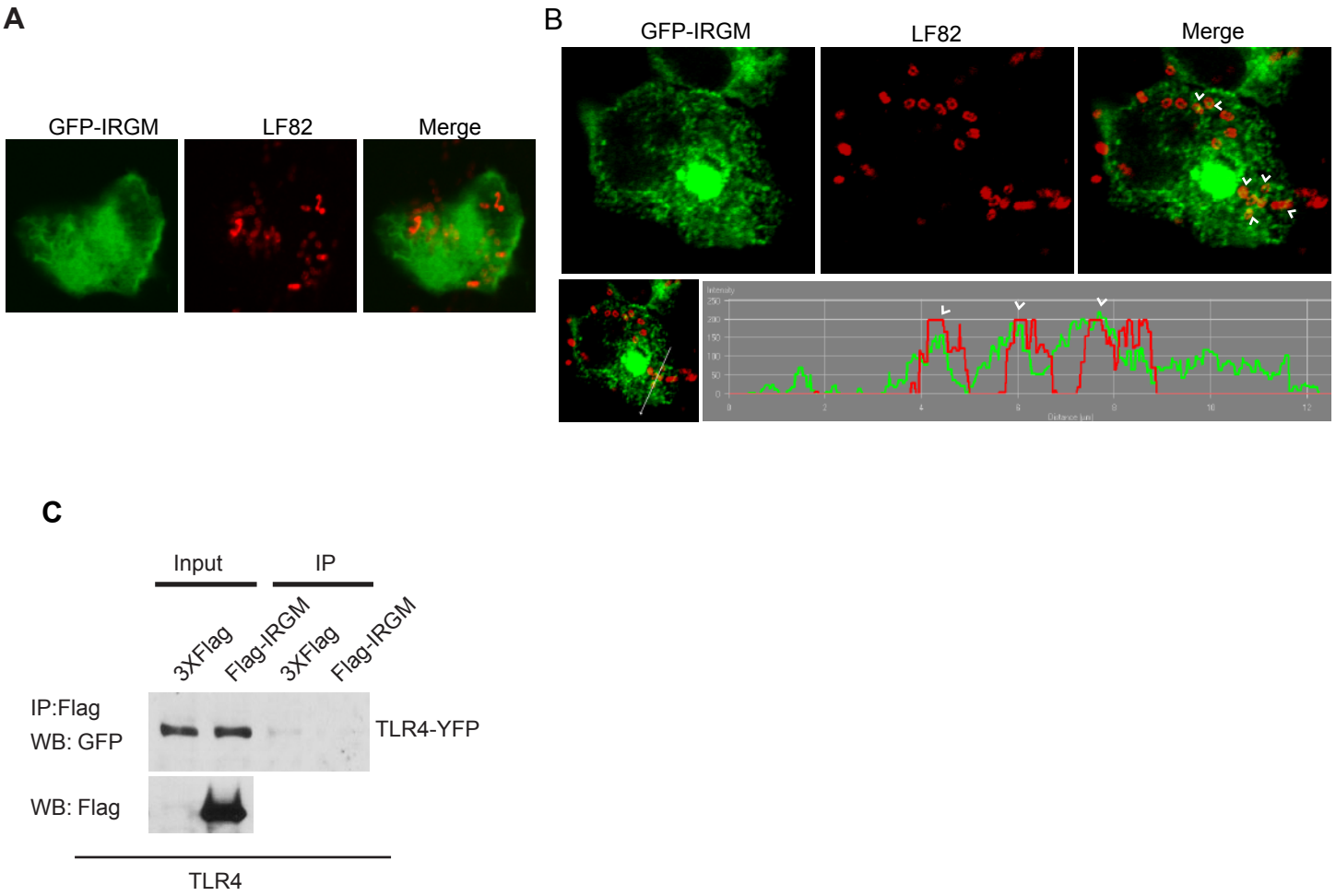

Figure S7, related to Fig. 7. Ubiquitination of IRGM is important for its anti-microbial function . (**A**) Representative confocal images of GFP-IRGM transfected HEK293T cells infected with invasive *E. coli* LF82 (red, LPS antibody). (**B**) Representative confocal images of GFP-IRGM- and Flag-NOD2-co-transfected HEK293T cells infected with invasive *E. coli* LF82 (red, LPS antibody). Bottom panel, co-localization profile tracing along straight line using LSM510 software. (**C**) Lysates of cells co-expressing control vector or Flag-IRGM and GFP-TLR4 were subjected to immunoprecipitation with anti-Flag and blots were probed with indicated antibodies (WB).

Supplemental Experimental Procedures

Cell culture

Cell lines were maintained and primary human peripheral blood-monocyte-derived macrophages were isolated and maintained as described (Gutierrez et al., 2004).

Transfections

Plasmid transfections in HEK293T were performed using ProFection Mammalian Transfection System from Promega; siRNAs were delivered to cells by nucleoporation (Amaxa).

Microscopy analyses and quantification

Immunofluorescence was performed as described earlier (Kyei et al., 2009). For quantification of puncta, images from different fields were captured and analyzed. For quantification of total cell fluorescence, image J was used as described previously (Chauhan et al., 2013).

Gene expression analysis

Total RNA was isolated from cell culture using Trizol as per the manufacturer's instruction (Invitrogen). For quantitative real-time PCR: TURBO DNA-free kit (Ambion) was used to remove contaminating residual DNA; cDNA was prepared using the high capacity cDNA reverse transcription kit as per the manufacturer's instruction (Applied Biosytem). Taqman probes (Applied Biosystem) and real-time PCR master mixes (Applied Biosystem) were used for real-time PCR as per the manufacturer's instruction. Data were normalized using GAPDH.

Cytokine and NF-kB responses

For NFkB-p65 nuclear localization assay, HeLa cells were platted on cover slips a day before infection. Cells were infected with AIEC LF82 strain at MOI of 1:20 for 2 h followed by washings with PBS and fixing the cells with 4% paraformaldehyde. Cells were visualized using a laser confocal microscope and images were captured using LSM510 software. For IL-1β measurement, IL-1β transcription was determined using qRT-PCR in THP-1 cells.

Bacterial survival analyses

AIEC LF82 survival assay was performed as described previously (Lapaquette et al., 2010). HEK293T cells were infected with AIEC LF82 of MOI of 1:20 for 3 h. Cells were treated with gentamycin (100 µg/ml) for 1 h followed by incubation in fresh media for 2 h. Cells were lysed and surviving bacteria quantified by plating and determining colony forming units.

Proximity ligation assay (PLA)

HEK293T cells transiently expressing the plasmid constructs were fixed and PLA (Soderberg et al., 2006) performed according to the manufacturer’s protocol (Olink Bioscience). Samples were then imaged and analyzed by high content microscopy using a CellomicsArrayScan (Thermo Scientific) with images analyzed using pre-set parameters for cell and PLA puncta identification within iDev software (Thermo Scientific). The average total area of red PLA puncta was determined per cell for a minimum of 500 GFP-IRGM positive cells.

Flag pull-down assay

Lysates of HEK293T cells transiently expressing the Flag-NOD2 constructs were incubated with anti-Flag magnetic beads (Sigma) for 2 h. Beads were washed thoroughly (5X) to remove unbound contaminants. The collected beads were incubated with purified recombinant proteins (GST or GST-IRGMd (Singh et al., 2010)) for 2 h and then washed again (5X). The beads were boiled in SDS-PAGE buffer and subjected to Western blotting

Supplemental References

Chauhan, S., Goodwin, J.G., Manyam, G., Wang, J., Kamat, A.M., and Boyd, D.D. (2013). ZKSCAN3 is a master transcriptional repressor of autophagy. Molecular cell *50*, 16-28.

Gutierrez, M.G., Master, S.S., Singh, S.B., Taylor, G.A., Colombo, M.I., and Deretic, V. (2004). Autophagy is a defense mechanism inhibiting BCG and Mycobacterium tuberculosis survival in infected macrophages. Cell *119*, 753-766.

Kyei, G.B., Dinkins, C., Davis, A.S., Roberts, E., Singh, S.B., Dong, C., Wu, L., Kominami, E., Ueno, T., Yamamoto, A.*, et al.* (2009). Autophagy pathway intersects with HIV-1 biosynthesis and regulates viral yields in macrophages. The Journal of cell biology *186*, 255-268.

Lapaquette, P., Glasser, A.L., Huett, A., Xavier, R.J., and Darfeuille-Michaud, A. (2010). Crohn's disease-associated adherent-invasive E. coli are selectively favoured by impaired autophagy to replicate intracellularly. Cell Microbiol *12*, 99-113.

Singh, S.B., Ornatowski, W., Vergne, I., Naylor, J., Delgado, M., Roberts, E., Ponpuak, M., Master, S., Pilli, M., White, E.*, et al.* (2010). Human IRGM regulates autophagy and cell-autonomous immunity functions through mitochondria. Nat Cell Biol *12*, 1154-1165.

Soderberg, O., Gullberg, M., Jarvius, M., Ridderstrale, K., Leuchowius, K.J., Jarvius, J., Wester, K., Hydbring, P., Bahram, F., Larsson, L.G.*, et al.* (2006). Direct observation of individual endogenous protein complexes in situ by proximity ligation. Nature methods *3*, 995-1000.